X-ray multielectronic photoexcitations near the K edge of xenon

Moshe Deutsch
Physics Department, Bar-Ilan University, Ramat-Gan 52900, Israel
and Division of Applied Sciences, Harvard University, Cambridge, Massachusetts 02138

Peter Kizler
Hamburger Synchrotronstrahlungslabor at Deutsches Elektronen-Synchrotron, D-2000 Hamburg 52, Federal Republic of Germany
(Received 16 July 1991; revised manuscript received 26 August 1991)

The near-K-edge x-ray photoabsorption spectrum of xenon was measured using synchrotron radiation. Several simultaneous two-electron excitation features were detected. Their identification is supported by nonrelativistic and relativistic energy-level calculations. The relative cross sections extracted from the data are consistent with previous measurements on Kr. Relativistic sudden-approximation-shake-theory cross sections are found to overestimate the measured ones by factors of 2–3, but closely follow level-dependent trends in the measured data.

PACS number(s): 32.30.Rj, 32.80.Hd

Simultaneous multielectronic excitations in an atom can provide, in principle, information on intershell and intrashell correlations [1,2]. A method of choice for probing these excitations are near-edge photoabsorption measurements, which yield direct energy-level and cross-section information, provided that monatomic gaseous samples are used. In solids, liquids, and even gases of multiatomic molecules, the weak multielectronic features are masked by the much larger x-ray absorption near-edge structures (XANES's) and extended x-ray-absorption fine structures (EXAFS's) dominating the spectrum in this energy range [3]. Of the noble gases, the natural candidates for such measurements, the K edges of neon [4], argon [5], and krypton [6–8] were measured with high resolution, showing a rich spectrum of two- and three-electron excitations as well as important details of the underlying one-electron ($1e$) spectra. These spectra, and in particular the Ar one, were used in a number of theoretical studies to test models for the excitation dynamics and the relative importance of effects such as postcollisional interaction, relaxation, and exchange [2,9–11]. Saha's [12] recent multiconfigurational Hartree-Fock (HF) calculations for Ar reproduced accurately the $1e$ cross section and the energies of the major two-electron ($2e$) excitations. His $2e$ cross sections, however, considerably overestimate the observed values. Deutsch and Hart [6–8] found the measured cross sections for $2e$ $1snl$ excitations in both Kr and Ar to be much smaller than predicted theoretically by Carlson and Nestor (CN) [13] for outer nl electrons, with the agreement becoming progressively better for the inner ones. The ratios of several $2e$ cross sections, however, were found to be in good agreement with the predictions of shake theory [14,15].

For the Xe K edge, the only measurement available is that of Holland *et al.* [16]. This, however, has limited range and resolution, and was not analyzed for multielectronic effects. Our very recent absolute cross-section measurements in this energy range [17] show the significant (~10%) relativistic and relaxational effects predicted theoretically for the $1e$ cross section [18]. We present here the results of a study of the $1snl$ $2e$ excitation spectrum of xenon using synchrotron x-ray photoabsorption. The cross sections are found to depend weakly on n and l and are smaller than predicted theoretically for the outer electrons, in accord with the results obtained for Ar and Kr. Nonrelativistic Hartree-Fock (HF) and relativistic Dirac-Fock (DF) energy-level calculations are also presented. The DF results agree with, while the HF mostly underestimate, the predictions of the $Z+1$ approximation [19]. Partial agreement is found with shake theory concerning the nl dependence of the cross sections.

The measurements were done on 99.995%-pure Xe gas at the RÖMO II station at HASYLAB, in a standard transmission EXAFS configuration, with an energy resolution of $\Delta E/E \leq 5\times 10^{-4}$. For further experimental details see Ref. [17]. The energy scale was calibrated [17,20–21] using the best available experimental K-level energy, $E_K = 34\,565.4$ eV, derived from recent precision Xe $K\alpha_{1,2}$ [22] and Xe $L_{2,3}$ level [20] measurements.

The measured absolute K-excitation cross section is shown in Fig. 1. The higher-shell contributions were subtracted using the Victoreen formula [23], fitted to the data below the edge. The magnitude and shape of the major $1e$ contribution to the edge are discussed in detail elsewhere [17]. Note, however, that the prethreshold $1e$ $1s\rightarrow nl$ resonances, so prominent in Ar and Ne, are not observed here. This is due to the considerable overlap of the lines, caused by their large lifetime widths [24], ~12 eV, and their small separation, 1–2 eV, as derived from the Cs I optical spectrum [25], using the $Z+1$ approximation, which places the onset of the $1s$ continuum only 2.4 eV above the lowest-lying resonance $1s\rightarrow 6p$. This behavior closely resembles that previously measured for krypton in the corresponding energy range [8] where the lifetime widths, ~3 eV, are also larger than the 1–2-eV separation of the individual resonances. The very large

lifetime width of the K level in xenon smears out the $2e$ edges as well, and renders their identification in the data considerably more difficult than for the lower-Z noble gases. Consequently, the only $2e$ feature visible on the scale of Fig. 1 is a broad shoulder whose threshold is at ~ 70 eV. The $1e$ background contribution, which peaks at ~ 25 eV and then decreases, creates, along with the increase at ~ 70 eV due to the onset of the $2e$ excitations, the dip seen in Fig. 1 at ~ 70 eV. The shoulder is identified by the energy-level calculations as the onset of the $1s4d$ excitation. As no fine structure was resolved in the $2e$ features, the energy-level calculations were done for the lowest-lying allowed transitions, which are necessarily bound-bound ones. The relativistic DF energy levels, discussed below, are shown in Figs. 1 and 2.

To obtain a better view of the small $2e$ features, one usually subtracts off all other contributions, using a chosen function fitted to the data *below* the threshold of the relevant feature. In our case, however, such a procedure is bound to be rather inaccurate due to the large lifetime width smearing, the highly nonlinear $1e$ cross section near the edge, and our poor knowledge of its exact shape [17]. We have, therefore, chosen to divide the data by a straight line fitted to the measured spectrum in the range 270–350 eV, where no $2e$ features were predicted, nor indeed found, and where the data were found to be highly linear and smooth. This normalized spectrum was then lightly smoothed by three-point averaging, ensuring that no artifacts were introduced. The final result is shown in Fig. 2. As no fine structure was resolved in any of the features due to a particular pair of $1snl$ electrons, we felt a measure of justification for regarding the total complex of expected transitions involving this pair as a steplike structure in the cross section, similar to a conventional $1e$ absorption edge. Thus the normalization procedure outlined above is expected schematically to show a lifetime-width-smeared "staircase," with step contributions from the various $2e$ transitions, superimposed on the $1e$ cross section. Figure 2 indeed displays the expected "smeared staircase" from ~ 70 eV on. The sharp peak at ~ 25 eV and the fast-decreasing cross section on its high-energy side reflect mainly the shape of the $1e$ cross section, with some possible contributions from the $1s5p$, and to a smaller extent $1s5s$, excitations. The onset A of the lowest $1s4d$ excitation, $1s4d \rightarrow 6s6p$, is now clearly visible. The j splitting of the $4d$ electrons, ~ 2.5 eV, is too small to be resolved. However, the weak feature marked B, ~ 12 eV above A, may be attributed to the onset of the doubly ionized $[1s4d]$ continuum, which we calculated to be 11.9 eV above the $[1s4d]6s6p$ level. The onset of the $1s4p$ excitations C, though unambiguous, is much less visible than the $1s4d$ one. The much-weaker and less-definite feature D can be associated with the onset of the j-split $1s4p$-excitation and the double-ionization $[1s4p]$ threshold, calculated to be 13.6 and 13.0 eV, respectively, above the lowest $1s4d$ excitation. Finally, E at ~ 230 eV marks the opening of the $1s4s$ excitation channel. The small magnitude of D and E renders their identification difficult and by no means unambiguous. The $1s5p$ and $1s5s$ edges are located at very inconvenient regions of the spectrum. The fast-increasing slope at the position of the former, and the small magnitude expected for, as well as the large intensity changes at the position of the latter, all due to the underlying $1e$ spectrum, defied our efforts to obtain a clear indication of their onset and size. The procedures detailed above were also used to search for the $1s3l$ higher-energy edges. However, within the limits of our experimental accuracy listed in Table I, no indications for these edges were detected in the data.

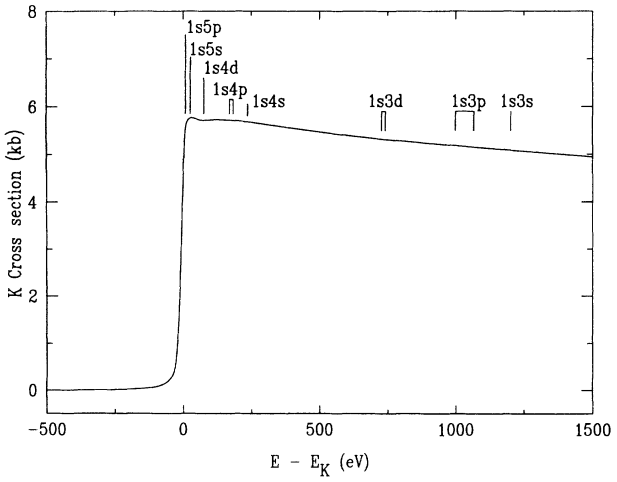

FIG. 1. Measured absolute K cross section for Xe. The energy scale is relative to the onset of the $1s$ continuum at $E_K = 34\,565.4$ eV. The energy levels were calculated using the relativistic DF method.

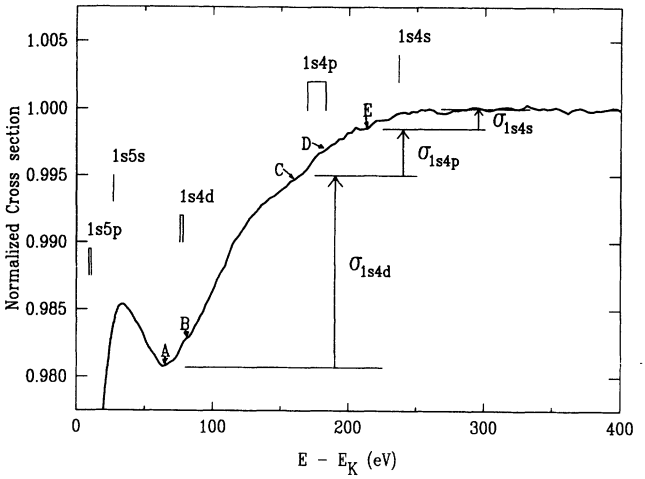

FIG. 2. The near-edge cross section, normalized by a straight line fitted to the data of Fig. 1 in the region 270–350 eV. Energy levels are relativistic DF ones. The two-electron edges visible in the figure are marked by characters and discussed in the text. A schematic separation into individual cross sections is also shown.

The measurements were supplemented by nonrelativistic HF [26] and relativistic DF [27] energy-level calculations. The calculated lowest-lying bound-bound transition energies are given in Table I. The <0.1 eV j splitting of the $6p$ level was neglected in the DF calculations, and all HF levels are j averaged. The DF levels are also

TABLE I. Energy levels obtained from HF and DF calculations and optical and vuv measured Cs data in the $Z+1$ approximation. All energies are in eV units. The lower member of a j doublet is denoted by a dash. Hole states are enclosed in square brackets. The cross sections, relative to that of the single $1s$ electron, σ/σ_K, as obtained from our measurements and from theory, are also listed. The estimated errors in the former are ±20%

Xe	ΔE		Cs $Z+1$ Approx.		$10^3\sigma/\sigma_K$	
Config.	DF	HF	Config.	ΔE[a]	Meas.	CN[b]
$[1s]$	0	0	$5p^6$	0	1000	1000
$[1s5p]6s^2$	9.2	10.0	$[5p]6s^2$	8.41*		83.9
$[1s5p\text{-}]6s^2$	10.8		$[5p\text{-}]6s^2$	9.63*		37.3
$[1s5s]6s6p$	27.0	25.4	$[5s]6s6p$	(22.7)		16.7
$[1s4d]6s6p$	76.0	80.4	$[4d]6s6p$	79.39	14	24.6
$[1s4d\text{-}]6s6p$	78.3		$[4d\text{-}]6s6p$	81.63		16.5
$[1s4p]6s^2$	169.4	170.4	$[4p]6s^2$	161.28	3.7	7.3
$[1s4p\text{-}]6s^2$	183.0		$[4p\text{-}]6s^2$	172.5		3.7
$[1s4s]6s6p$	236.7	221.6	$[4s]6s6p$	(230.8)	1.2	2.3
$[1s3d]6s6p$	727.3	748.1	$[3d]6s6p$	(725.5)	≤0.5	3.2
$[1s3d\text{-}]6s6p$	741.2		$[3d\text{-}]6s6p$	(739.5)		2.2
$[1s3p]6s^2$	999.5	996.9	$[3p]6s^2$	(997.6)	≤0.3	2.2
$[1s3p\text{-}]6s^2$	1066.4		$[3p\text{-}]6s^2$	(1065.5)		1.1
$[1s3s]6s6p$	1202.6	1127.8	$[3s]6s6p$	(1217.1)	≤0.3	0.73

[a]Reference [28] except those values marked by an asterisk (Ref. [25]) and in parentheses (Ref. [29]).
[b]CN, Ref. [13].

marked in Fig. 2 and seem to be reasonably well aligned with the admittedly rather broad $2e$ edges. As the differences between the HF and DF levels are smaller than the widths of the $2e$ edges, no conclusions can be drawn from the data on the importance of relativistic effects in these transitions. Table I also lists levels derived from optical [25] and vacuum-ultraviolet (vuv) [28] measurements on Cs using the $Z+1$ approximation. Where data for the lowest-lying resonances were not available, edge values [29] for the corresponding doubly ionized states are listed. The neutral resonance levels are a few eV *lower* than the corresponding ionization thresholds. The actual thresholds, however, are *higher* by a few eV than the values of Ref. [29], as pointed out by Deslattes and Kessler [22]. Since these two opposing corrections are roughly of the same magnitude, the bracketed values are expected to approximate the listed resonance levels well. Except for the $1s5s$ and $1s4d$, where the differences are marginal (a few eV) and the $1s4p$, where a 8–10-eV difference is observed, the $Z+1$ data agree rather well with the DF results and significantly less well with the HF ones. The edge values [29] for the $1s4d$ transitions, 76.5 and 78.8 eV, further enhance this agreement. Thus, the $Z+1$ approximation still retains some usefulness for spectral feature identification. The ~3-eV discrepancy between the edge [29] and vuv values for $1s4d$ is, however, puzzling, in particular since their $1s4p$ values agree to within 0.1 eV.

The $2e$ relative cross sections $\sigma_{1snl}/\sigma_{1s}$ were approximated from the measured data by the admittedly somewhat arbitrary but previously employed [7,30] procedure of taking the ratios of the jumps at the relevant edges. In our case, however, the accuracy of this procedure is further limited by the fast, and poorly known, variation of the underlying $1e$ background and the large lifetime and resolution smearing. The jump ratios derived from the data are listed in Table I. The estimated errors in these values are ±20%. For the undetected $1s3l$ excitations, the upper limits, derived from the estimated random measurement error, are listed. We also list the shake-theory predictions of CN, which, though fairly old by now and neglecting important relaxation and correlation effects, are the only published $2e$ cross-section calculations for xenon, to the best of our knowledge. The three measured cross sections are smaller than the calculated ones by a factor of 2–3. This discrepancy is considerably smaller than that in the equivalent $1s3l$ levels of Kr, which ranges from [7] 2 to 18. However, the *ratios* of the

various $1s4l$ cross sections of Xe, 0.08:0.26:1, are close to the 0.06:0.27:1 calculated by CN. The good agreement of the ratio of the $1sns/1snp$ cross sections here and in Kr does not support an enhanced Coster-Kronig depopulation of the $1sns$ hole states to $1snp$ ones, in contrast to Ar, where this process was suggested [5] to account for the absence of $1s3s$ features. Furthermore, the measured $1s4s$ and $1s4p$ cross sections of Xe are equal, within their combined experimental error, to the measured equivalent $1s3s$ and $1s3p$ ones in Kr. This is, again, in full accord with the CN calculations. Note, however, that there is a large discrepancy in the ratio of cross sections for the $1snd$ excitations in the two atoms; measurement yields 1:7, while CN calculate 1:1.2. Not surprisingly, the agreement with the results of the CN theory seem therefore to be only partial. The discrepancy is probably due to the CN's use of the sudden approximation, which is valid only far from threshold. Near-threshold relaxation and correlation effects lower the cross section for shake-off, and to a small extent also shakeup, processes [31]. Calculations taking these effects into account should therefore improve the agreement with our measured cross sections. On the experimental side, high-resolution photoelectron spectroscopy, a technique well suited to the problem at hand, would be an ideal way to obtain further information on the multielectronic processes studied here.

We gratefully acknowledge beam-time allocation and the kind assistance of the staff at HASYLAB, DESY, Hamburg, important comments by G. Materlik, and expert programming by G. Zipori. This work was supported by The Fund for Basic Research of The Israel Academy of Sciences and Humanities.

[1] W. Jitschin, in *Progress in Atomic Spectroscopy D,* edited by H. J. Beyer and H. Kleinpoppen (Plenum, New York, 1987), p. 295.
[2] J. W. Cooper, Phys. Rev. A **38**, 3417 (1988).
[3] R. Frahm, W. Drube, I. Arcon, D. Glavic, M. Hribar, and A. Kodre, in *Proceedings of the Second European Conference on Progress in X-Ray Synchrotron Radiation Research,* edited by A. Balerna, E. Bernieri, and S. Mobilio (Italian Physical Society, Bologna, 1990), p. 129.
[4] J. M. Esteva, B. Gauthe, P. Dhez, and R. C. Karnatak, J. Phys. B **16**, L263 (1983).
[5] R. D. Deslattes, R. E. Lavilla, P. E. Cowan, and A. Henins, Phys. Rev. A **27**, 923 (1983).
[6] M. Deutsch and M. Hart, Phys. Rev. Lett. **57**, 1566 (1986).
[7] M. Deutsch and M. Hart, Phys. Rev. A **34**, 5168 (1986).
[8] M. Deutsch and M. Hart, J. Phys. B **19**, L303 (1986).
[9] J. Tulkki and T. Åberg, J. Phys. B **18**, L489 (1985).
[10] S. C. Vinayagam and K. D. Sen, Phys. Rev. A **36**, 2971 (1987).
[11] V. L. Sukhorukov *et al.*, J. Phys. (Paris) **48**, 1677 (1987).
[12] H. P. Saha, Phys. Rev. A **42**, 6507 (1990).
[13] T. A. Carlson and C. W. Nestor, Phys. Rev. A **8**, 2887 (1973).
[14] T. Åberg and G. Howat, in *Handbuch der Physik,* edited by W. Melhorn (Springer, Berlin, 1984), Vol. 31.
[15] T. A. Carlson *et al.*, Phys. Rev. **169**, 27 (1968).
[16] B. W. Holland, J. B. Pendry, R. F. Pettifer, and J. Bordas, J. Phys. C **11**, 633 (1978).
[17] M. Deutsch, G. Brill, and P. Kizler, Phys. Rev. A **43**, 2591 (1991).
[18] J. Tulkki, Phys. Rev. A **32**, 3153 (1985).
[19] I. Bergstrom and R. D. Hill, Ark Fys. **8**, 21 (1954); J. P. Briand *et al.*, J. Phys. B **9**, 1055 (1976); M. Deutsch, Phys. Rev. A **39**, 3956 (1989).
[20] M. Breinig, M. H. Chen, G. E. Ice, F. Parente, and B. Crasemann, Phys. Rev. A. **22**, 520 (1980).
[21] O. Keski-Rahkonen, G. Materlik, B. Sonntag, and J. Tulkki, J. Phys. B Phys. **17**, L121 (1984); T. Watanabe, Phys. Rev. **139**, A1747 (1965).
[22] R. D. Deslattes and E. G. Kessler, in *Atomic Inner-Shell Physics,* edited by B. Crasemann (Plenum, New York, 1985).
[23] *International Tables for X-Ray Crystallography,* edited by C. H. Macgillavry and G. D. Rieck (Kynoch, Birmingham, 1968), Vol. III, Chap. 3.2.
[24] M. O. Krause and J. H. Oliver, J. Phys. Chem. Ref. Data **8**, 329 (1979).
[25] C. E. Moore, *Atomic Energy Levels,* Natl. Bur. Stand. (U.S.) Circ. No. 467 (U.S. GPO, Washington, DC, 1968), Vol. III.
[26] C. Froese Fischer, Comput. Phys. Commun. **14**, 145 (1978).
[27] I. P. Grant *et al.*, Comput. Phys. Commun. **21**, 207 (1980).
[28] H. Petersen, K. Radler, B. Sonntag, and R. Haensel, J. Phys. B **8**, 31 (1975).
[29] J. A. Bearden and A. F. Burr, Rev. Mod. Phys. **39**, 126 (1967).
[30] S. I. Salem and A. Kumar, J. Phys. B **19**, 73 (1986), and references cited therein.
[31] J. Bradley Armen *et al.*, Phys. Rev. Lett. **54**, 182 (1985).